Storylines of Maritime Continent dry period precipitation changes under global warming

Article

Published Version

It is advisable to refer to the publisher's version if you intend to cite from the work. See Guidance on citing.

CentAUR

Central Archive at the University of Reading

Reading's research outputs online

ENVIRONMENTAL RESEARCH
LETTERS

LETTER • OPEN ACCESS

Storylines of Maritime Continent dry period precipitation changes under global warming

To cite this article: Rohit Ghosh and Theodore G Shepherd 2023 *Environ. Res. Lett.* **18** 034017

View the article online for updates and enhancements.

ENVIRONMENTAL RESEARCH
LETTERS

Storylines of Maritime Continent dry period precipitation changes under global warming

Rohit Ghosh[*] and Theodore G Shepherd

Department of Meteorology, University of Reading, Reading, United Kingdom
[*] Author to whom any correspondence should be addressed.

E-mail: r.ghosh@reading.ac.uk

Abstract

The dry half of the year from May to October over the Maritime Continent (MC) has experienced unprecedented damages from forest fires in recent decades. The observed interannual rainfall variability during this period is closely tied to sea surface temperature (SST) variability over the equatorial Pacific (EP). Therefore, the future evolution of EP SST can be expected to influence the climatological precipitation over the MC. Whilst multi-model means (MMMs) suggest a future drying trend over the south-western part of the MC, there is considerable model uncertainty. Here, using a storyline approach with the 38 climate models from Coupled Model Intercomparison Project Phase 6, we distinguish the model uncertainty associated with changes in the zonal EP SST gradient from that associated with the basin-wide EP (BEP) warming. We find that an increase in east-to-west EP SST gradient would bring more rainfall over the north-eastern regions including northern Borneo, Sulawesi and New Guinea. In contrast, the intensity of the basin-wide warming of EP SST is directly linked with the drying response seen over the south-western MC in the MMM. This drying affects the highly vulnerable regions of Sumatra and Kalimantan for forest fires. Our results suggest that a storyline under higher BEP warming accompanied by an El-Niño like change in zonal SST gradient would lead to even drier climatic conditions over these key regions. However, the observed record of more than one hundred years favours a storyline of lower BEP warming accompanied by a La-Niña like change in zonal SST gradient, which would lead to minimal drying over the south-western MC and wetter conditions over the north-eastern parts of the MC.

1. Introduction

The Maritime Continent (MC) region mainly consists of the archipelagos of Indonesia and receives rainfall year round, with a wet half and a comparatively dry half of the year (Murakami and Sumi 1978, Hendon 2003, McBride *et al* 2003, Chang *et al* 2004, 2005). The minimum rainfall during the dry half (from May to October) occurs in August and the rainfall during this period is found to be closely tied to variability in equatorial Pacific (EP) sea surface temperature (SST), especially the El Niño Southern Oscillation (Haylock and McBride 2001, Hendon 2003, McBride *et al* 2003, Juneng and Tangang 2005, Kubota *et al* 2011, Lestari *et al* 2016, Zhang *et al* 2016, Supari *et al* 2018). A growing number of forest and peat fire events have been recorded over a vast region

of the MC during this dry period over the last decades (Nichol 1998, Koplitz *et al* 2016). These fires bring a large amount of smoke and haze over the human population and cause severe distress to human health, leading to high mortality (Johnston *et al* 2012, Kim *et al* 2015, Lelieveld *et al* 2015, Koplitz *et al* 2016). The most devastating haze from fires and associated high casualties mainly occur during the years with a strong El Niño (Tangang *et al* 2010, Reid *et al* 2012, Marlier *et al* 2013). The severe haze in the 2015 strong El Niño year took an estimated 91600 lives in Indonesia alone (Koplitz *et al* 2016). Hence it is of huge concern how much damage such events could bring under changing climatic conditions over the MC.

Previous studies from a few global and mostly regional climate models show a drying in multi-model mean (MMM) climate changes over

the southern and western Sumatra and Kalimantan regions of the MC (Giorgi *et al* 2019, Kang *et al* 2019, Supari *et al* 2020, Tangang *et al* 2020, Ge *et al* 2021). These are the regions that have shown high vulnerability of having large fire events in strong El Niño years (Page *et al* 2002, Huijnen *et al* 2016). However, an extensive study with the large number of global models from the latest Coupled Model Intercomparison Project Phase 6 (CMIP6) shows uncertainty in climatological precipitation changes over those regions (Zappa *et al* 2021). Given that EP SST is one of the main drivers of variability in MC dry period precipitation, this uncertainty in projected precipitation changes could be due to different patterns of evolution of EP SST in different models. A recent study has shown that in the CMIP5 models the EP SST indeed evolves differently in different models, with more models showing a larger warming of eastern EP (EEP) SST than of western EP (WEP) SST, and with different magnitudes of overall warming of the basinwide EP (BEP) (Yang *et al* 2021). This model uncertainty motivates us to examine how the changes in the patterns of EP SST influence the projected changes in dry-season precipitation over the MC. We address this question using the storyline approach (Shepherd *et al* 2018), previously developed to explain changes in midlatitude precipitation in terms of remote drivers (Zappa and Shepherd 2017, Mindlin *et al* 2020), but now using EP SST patterns as the remote drivers.

2. Data and methods

To understand what drives future changes in MC dry season (May-to-October, hereafter MJJASO) precipitation, we use simulations from 38 coupled climate models in CMIP6 (Eyring *et al* 2016, Ghosh 2023). The descriptions of all models used are given in supplementary table S1. Not all models provide multiple ensemble members. To simplify the analysis, we therefore only use one ensemble member from each model. This also helps in making a straightforward comparison of each model's climatology to the observations, which is also a single realisation of Earth's climate.

For constructing the climatology of past climate, we average the data from 1930 to 1960 in the historical simulations. We chose this period to minimise the prominent effect of natural forcings from volcanic eruptions on the estimate of global mean surface temperature (GMST), which can be seen after 1960 due to three major eruptions from Agung (1963), El Chichón (1982) and Pinatubo (1991) (Lewis and Curry 2015). The future climatology is determined by averaging the data from 2070 to 2100 in the SSP5-8.5 simulations, and the difference between the two is taken to represent the response of each model to climate change.

Following the method described in Zappa and Shepherd (2017), we perform a multiple linear regression (MLR) analysis where, for each grid point in the MC and for each climate model, the climatological change in the dry season precipitation (ΔP) is the dependent variable, and the two indices of SST evolution over the EP, identified by Yang *et al* (2021), are considered as the independent variables, i.e. they represent the presumed drivers of MC precipitation changes. One of these SST drivers is the change in BEP (150°E-90°W, 10°S-10°N) SST (ΔT_{BEP}); the other is the change in the SST difference between the western (155°E–175°W, 5°S–5°N) and eastern (145°W–115°W, 5°S–5°N) EP ($\Delta T_{WEP-EEP}$). To remove the confounding effects of different climate sensitivities in the different models, we scale both the precipitation and SST changes by the changes in GMST (ΔT_{GMST}). This step, which appeals to pattern scaling (Tebaldi and Arblaster 2014), is a reasonable assumption for transient scenarios such as SSP5-8.5 (especially for regions not influenced by the Arctic) and allows us to disentangle the uncertainty in the spatial pattern of precipitation response from the uncertainty in global warming. In particular, it allows us to explain the precipitation response in terms of the changes in the drivers, conditional on a given global warming level (Zappa and Shepherd 2017). All driver changes are standardised before applying the MLR. The MLR equation is expressed as:

$$\left(\frac{\Delta P}{\Delta T_{GMST}}\right)_m = a + b\left(\frac{\Delta T_{BEP}}{\Delta T_{GMST}}\right)'_m + c\left(\frac{\Delta T_{WEP-EEP}}{\Delta T_{GMST}}\right)'_m + e_m. \quad (1)$$

Here m is the index running over the different models; ΔP is the precipitation change at each grid point; b and c are the regression coefficient maps (i.e. functions of latitude and longitude) in units of mm d^{-1} K^{-1} change in GMST, which represent the response in the local precipitation from the two respective SST drivers; the constant factor a indicates the precipitation change without any anomalies in the drivers, i.e. the MMM response per Kelvin change in GMST; e_m is the residual for each model; and the primes denote standardised anomalies.

This approach is predicated on the hypothesis that the model uncertainty in the precipitation response is dominated by the model uncertainty in the driver responses with the precipitation response to those drivers assumed to be consistent between models. The success of the approach is assessed through metrics such as the fraction of variance explained, and the median absolute deviation of the residuals.

For comparison with observed climatology and variability, we use Global Precipitation Climatology

Center (GPCC) precipitation data at 1 degree horizontal resolution (Becker *et al* 2013, Schneider *et al* 2017) and Met Office Hadley Centre SST data for the period 1901–2019 (Rayner *et al* 2003). An empirical orthogonal function (EOF) analysis is performed to capture the first two modes of SST variability over the tropical Pacific.

3. Results

3.1. Climatology: observations and CMIP6

We first compare the climatology in the models with observations for the chosen historical period (1930–1960) to assess the extent to which the models are able to capture the large-scale characteristics of MC dry period precipitation (figure 1). Generally more rainfall is found to be concentrated over the islands compared to the surrounding oceans due to the seabreeze convergence over the islands (Qian 2008). The observed climatology shows one centre of maximum climatological precipitation of around 8–10 mm d^{-1} over north-western Borneo and another over New Guinea. The islands of Java and Sumatra also have rainfall in the range of 4–6 mm d^{-1}. The overall similarity of the large-scale historical climatological precipitation patterns indicates that the CMIP6 models are able to simulate the observed large-scale structure of the MC precipitation. This gives us confidence to investigate the future evolution of the large-scale precipitation climatology under global warming based on the CMIP6 models.

3.2. Observed association of dry period MC precipitation to EP SST

The observed record of the last 119 years can help understand how the interannual variability in EP SST relates to that of MC dry period precipitation. This understanding can be used to support the causal interpretation of the relationships across the climate model projections that are shown later from the MLR analysis. In this study, our two main drivers of the climatic changes are BEP SST change and the change in the zonal gradient of the EP SST (WEP-EEP SST). In the observations, both indices show a positive trend over the last century, indicating a moderate warming of the BEP with a comparatively larger warming of the WEP than the EEP (figure S1). The observed joint trend lies just within the spread of the historical trends simulated by the CMIP6 models, although the observed WEP-EEP SST trend is found at the extreme positive limit of the model simulated trends, potentially reflecting systematic model biases in capturing the EP SST gradient (Lee *et al* 2022, Wills *et al* 2022).

When we try to understand the observed precipitation response based on the interannual variability of these two drivers, they are found to be highly correlated due to the highly variable EEP region being a common part of both drivers' regions (not shown).
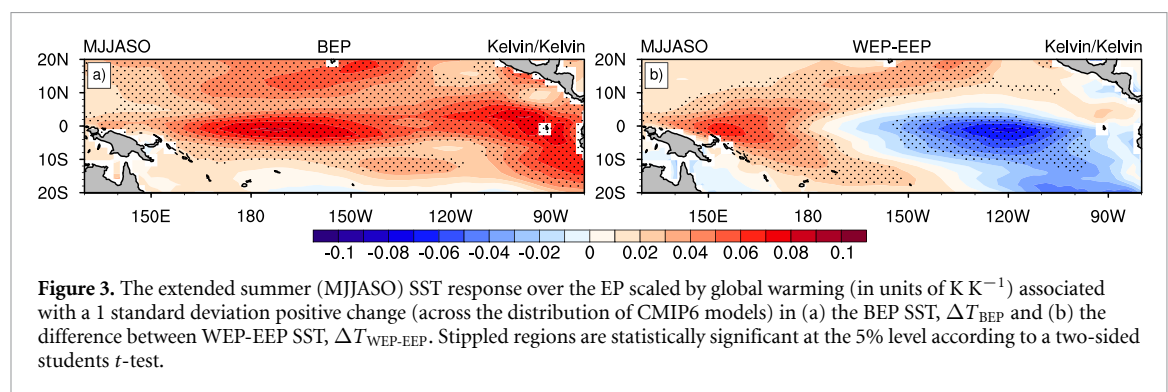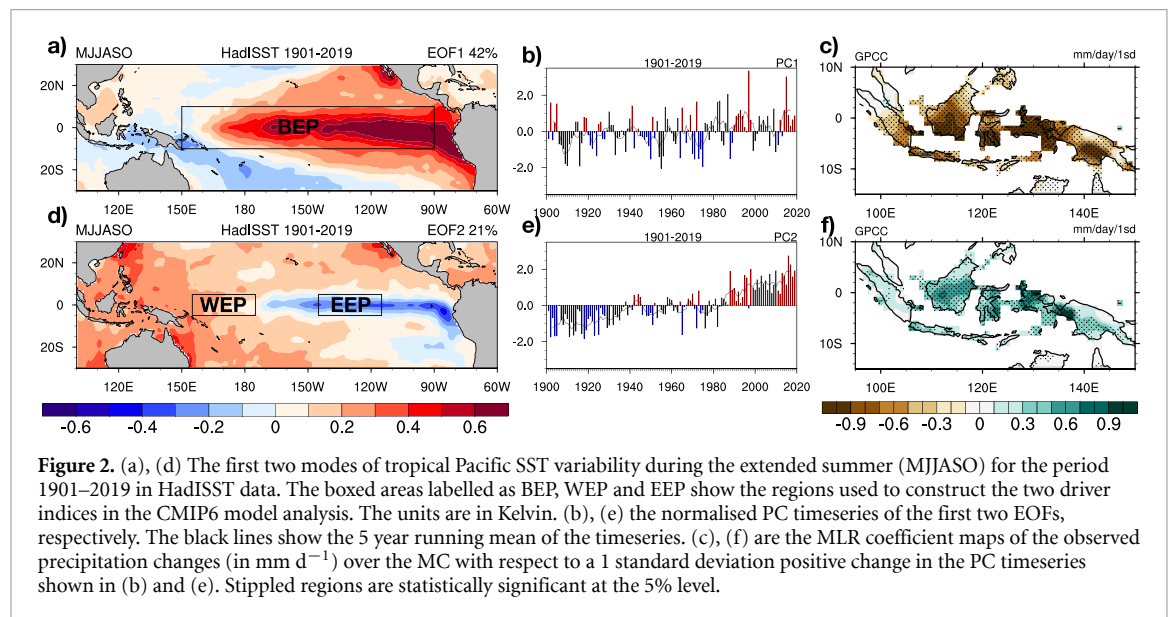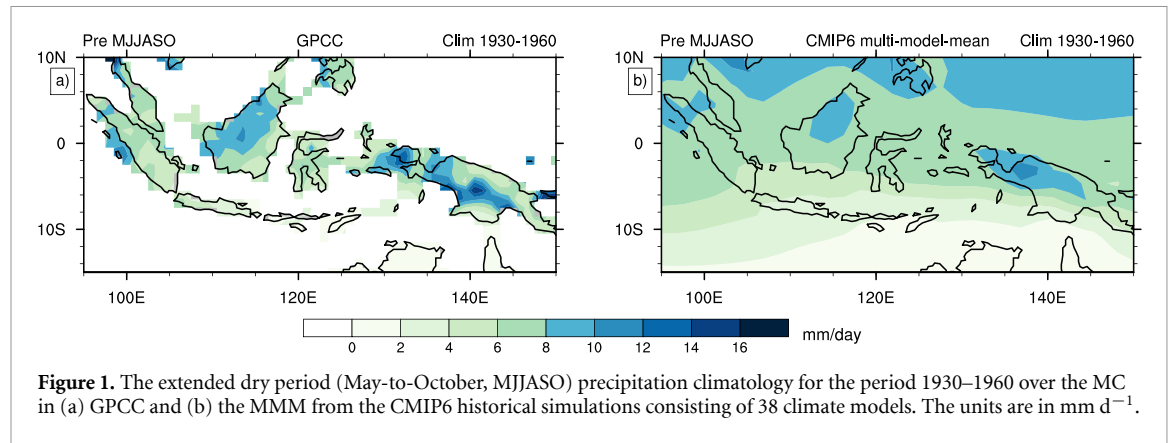
We address this through EOF analysis which separates the BEP warming and the zonal EP SST gradient (WEP-EEP SST) as the first two modes of tropical Pacific SST variability (figures 2(a) and (d)). The first mode shows a positive EP SST anomaly from the EEP to 150°W, which is similar to the BEP warming that is used as our first driver (shown as the black box in figure 2(a), representing the BEP region). This mode captures the moderate positive trend seen in the observed SST averaged over the BEP region (figure S1). The second mode has warm SST anomalies in the WEP, including the MC, and cold anomalies over the eastern to central EP. This mode is known as the 'Cold Tongue mode', whose PC shows a continuous upward trend throughout the 20th century, in contrast to the principal component (PC) of the first mode (figures 2(b) and (e)). This upward trend is suggested to be capturing the observed effect of global warming on the EP (Zhang *et al* 2010, L'Heureux *et al* 2013, Li *et al* 2015, 2017, Li *et al* 2019, Roxy *et al* 2019, Jiang and Zhu 2020).

An MLR analysis of the effect of these two tropical Pacific SST modes of variability on the observed MC dry period precipitation reveals an opposing influence (figures 2(c) and (f)). The first mode has a drying influence over most of the MC (figure 2(c)). In contrast, the second mode has a wetting influence over Borneo, Sulawesi and New Guinea, and a minimal influence over the island of Sumatra (figure 2(f)).

3.3. Future changes in EP SST drivers

We now seek to link the uncertainty in the MC dry period precipitation changes to the uncertainty in the EP SST changes in the CMIP6 models, as represented by the two driver indices ΔT_{BEP} and $\Delta T_{\text{WEP-EEP}}$. First, we visualize the spatial patterns of EP SST changes associated with the two drivers. Using the scaled SST changes at each grid cell as the dependent variable in equation (1), we obtain the spatial patterns of SST response associated with the driver responses (figures 3(a) and (b)). As expected from the definition of the driver indices, the pattern for ΔT_{BEP} (figure 3(a)) has a monopole structure across the EP, whilst that for $\Delta T_{\text{WEP-EEP}}$ has a dipole structure (figure 3(b)).

The uncertainty in the changes in these two drivers across the CMIP6 models, together with the uncertainty in global warming itself over the same period, are shown in figures 4(a) and (b). Note that panels a and b are separated because of the very different vertical scales in the two cases, since $\Delta T_{WEP-EEP}$ is a difference between two quantities. Yang *et al* (2021) has shown that the uncertainty in the CMIP5 models' unscaled $\Delta T_{WEP-EEP}$ response is uncorrelated with the uncertainty in their unscaled ΔT_{BEP} response. We find that in the CMIP6 models the unscaled driver responses have a correlation of 0.29, but after scaling

Figure 1. The extended dry period (May-to-October, MJJASO) precipitation climatology for the period 1930–1960 over the MC in (a) GPCC and (b) the MMM from the CMIP6 historical simulations consisting of 38 climate models. The units are in mm d^{-1}.

Figure 2. (a), (d) The first two modes of tropical Pacific SST variability during the extended summer (MJJASO) for the period 1901–2019 in HadISST data. The boxed areas labelled as BEP, WEP and EEP show the regions used to construct the two driver indices in the CMIP6 model analysis. The units are in Kelvin. (b), (e) The normalised PC timeseries of the first two EOFs, respectively. The black lines show the 5 year running mean of the timeseries. (c), (f) are the MLR coefficient maps of the observed precipitation changes (in mm d^{-1}) over the MC with respect to a 1 standard deviation positive change in the PC timeseries shown in (b) and (e). Stippled regions are statistically significant at the 5% level.

Figure 3. The extended summer (MJJASO) SST response over the EP scaled by global warming (in units of K K^{-1}) associated with a 1 standard deviation positive change (across the distribution of CMIP6 models) in (a) the BEP SST, ΔT_{BEP} and (b) the difference between WEP-EEP SST, $\Delta T_{WEP-EEP}$. Stippled regions are statistically significant at the 5% level according to a two-sided students t-test.

by global warming this correlation disappears (correlation coefficient = 0.01). We thus consider the two drivers as being independent. This simplifies the interpretation of the subsequent statistical analysis, although it is not a requirement for this methodology (see Mindlin *et al* 2020). Figure 4(c) shows the distribution of driver responses (scaled by global warming) across the CMIP6 models. In contrast to the historical period, where most of the models exhibit a positive WEP-EEP SST change, here less than one-third of the models do. This underscores the importance of

considering the full range of model possibilities rather than focusing on the MMM.

3.4. Future changes in MC dry period precipitation in relation to EP SST changes

The MLR analysis based on equation (1) reveals that a warmer BEP SST (larger IT$_{BEP}$) leads to drier conditions over the entire MC region (figure 5(a)). A prominent and significant drying response in the range of 0.10–0.15 mm d^{-1} K^{-1} can be seen over mid to southern Sumatra, Java, Kalimantan, and western
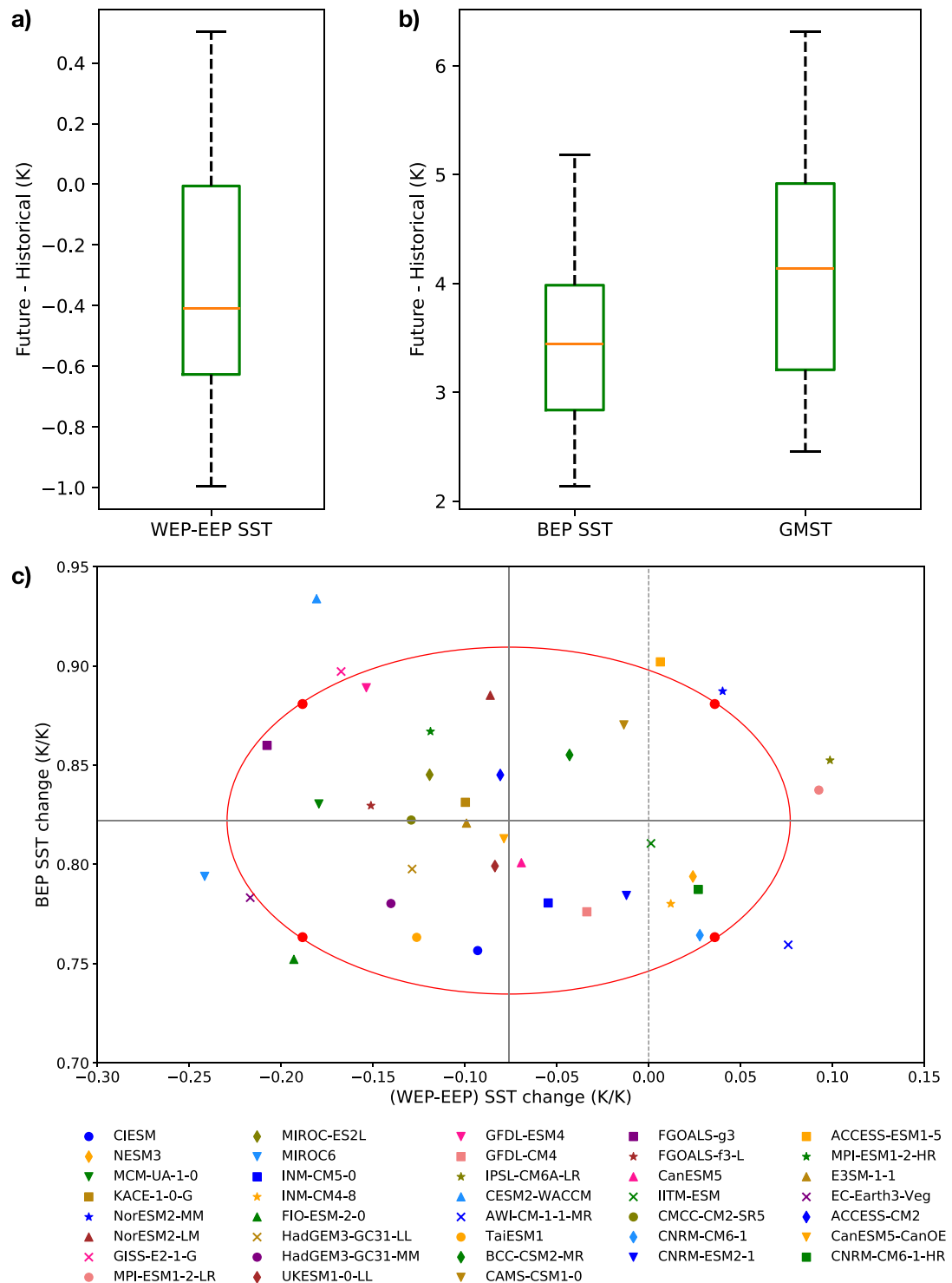
Figure 4. Distribution of the climate change response between the historical (1930–1960) and future (2070–2100) periods under SSP5-8.5 across 38 CMIP6 models in the extended summer period (MJJASO) for (a) the difference between western (155 E — 175 W, 5 S–5 N) and eastern (145 W–115 W, 5 S–5 N) EP SST ($\Delta T_{\text{WEP-EEP}}$), and (b) BEP SST (150 E — 90 W, 10 S–10 N, ΔT_{BEP}), and GMST (ΔT_{GMST}). The multi-model median (orange line), interquartile range (green box) and full spread (whiskers) are shown through a box-and-whiskers plot. (c) Scatter plot of ΔT_{BEP} (along the *y*-axis) and $\Delta T_{\text{WEP-EEP}}$ (along the *x*-axis), both scaled by ΔT_{GMST}, across the CMIP6 models. Each marker represents a particular model indicated in the legend. The dashed vertical line indicates the position of zero in the *x*-axis. The red ellipse shows the 80% confidence region from the bivariate normal distribution based on the CMIP6 model driver responses. The black vertical and horizontal lines show the means of the scaled driver responses, which divide the confidence ellipse into four equal quadrants. The red dots on the ellipse indicate the four storylines that combine anomalies in the two EP SST drivers.

Figure 5. MC dry period (MJJASO) precipitation response scaled by global warming (shaded, in mm d^{-1} K^{-1}) associated with a 1 standard deviation positive change (across the distribution of CMIP6 models) in (a) the BEP SST, and (b) the difference between WEP-EEP SST. Stippled regions are significant at the 5% level according to a two-sided students *t*-test. The vectors show the same but for the 850 hPa horizontal winds (in m s^{-1} K^{-1}). The length of a reference vector with magnitude 0.05 m s^{-1} K^{-1} is shown in the legend. The dashed boxes show specific regions considered in table 1.

to central New Guinea. The associated response in the 850 hPa wind shows diverging low-level wind anomalies associated with the centre of the drying. Among the drying regions, Sumatra and Kalimantan are the two regions which have seen devastating forest fires over the last decades (Page *et al* 2002, Margono *et al* 2014, Huijnen *et al* 2016). Meanwhile a positive change in the difference between WEP and EEP SST, indicating a larger warming over the warm pool region, leads to increased climatological precipitation across the central to north-eastern side of the MC (figure 5(b)). Specifically, northern Borneo, Sulawesi and New Guinea show a significant increase in climatological rainfall of around 0.15–0.20 mm d^{-1} K^{-1}. These wetter conditions are associated with converging low-level wind anomalies mainly coming from the WEP. We note that the regions of significant influence from these two EP SST drivers are somewhat complementary over the MC. The inferred precipitation responses to the two drivers are similar to those seen in the observations (figures 2(c) and (f)), giving confidence in their causality.

3.5. Storylines of future MC dry period precipitation changes

From the above analysis, four storylines of MC dry period precipitation change can be constructed following the methodology of Zappa and Shepherd (2017). Each storyline is based on a particular combination of the changes in the two drivers, BEP SST and WEP-EEP SST, compared to the MMM. We select equal standardised anomalies of the two drivers, which lie on the 80% confidence region of the joint distribution to represent possible but extreme storylines (shown as the four red dots on the 80% confidence ellipse in figure 4(c)), as the minimal set of possible combinations of positive and negative states that can be made from two drivers. From a Chi-squared distribution, that standardized amplitude is determined to be 1.26. Hence following equation (1), the four storylines are represented as:

$$\frac{\Delta P}{\Delta T_{GMST}} = \boldsymbol{a} \pm 1.26\,\boldsymbol{b} \pm 1.26\,\boldsymbol{c}. \qquad (2)$$

These four storylines are shown in figure 6, together with the MMM. Under a high BEP warming we find a prominent drying response over central to southern Sumatra and Java (figures 6(a) and (b)). The drying response extends further to southern Kalimantan and to the islands of Sulawesi in the case of a higher warming over the EEP, i.e. low (WEP-EEP) (figure 6(a)). In contrast, under a low BEP warming, we find a minimal drying response over the south-western MC (figures 6(d) and (e)). The MMM exhibits a drying response across the south-western part of the MC of a somewhat reduced amplitude compared to the high BEP warming storylines (figure 6(c)), which is consistent with the drying MMM response found in previous studies (Giorgi *et al* 2019, Supari *et al* 2020, Tangang *et al* 2020). Our analysis suggests that the MC drying seen in the MMM is linked with the amplitude of the BEP warming, and that a higher BEP warming would lead to a higher risk of increase in forest fires over the south-western part of the MC under global warming, for a given global warming level.

In the case of the storylines with high WEP-EEP SST change, we find a stronger and positive precipitation response over Borneo, Sulawesi and New Guinea (figures 6(b) and (e)). These storylines are worth highlighting as the observed record of SST changes shows a higher warming over the WEP over the last century (Seager *et al* 2019), even though a majority of the climate models project the opposite behaviour for the future (figures 4(a) and (c)).

Up to between 30% and 40% of the total variance in the MC dry period precipitation responses across the CMIP6 models is associated with the two EP SST drivers (figure S2). They explain more variance over the north-eastern parts compared to the south-western parts of the MC. Similar to Mindlin *et al* (2020), we compare the area averaged values of the precipitation changes in the four storylines over
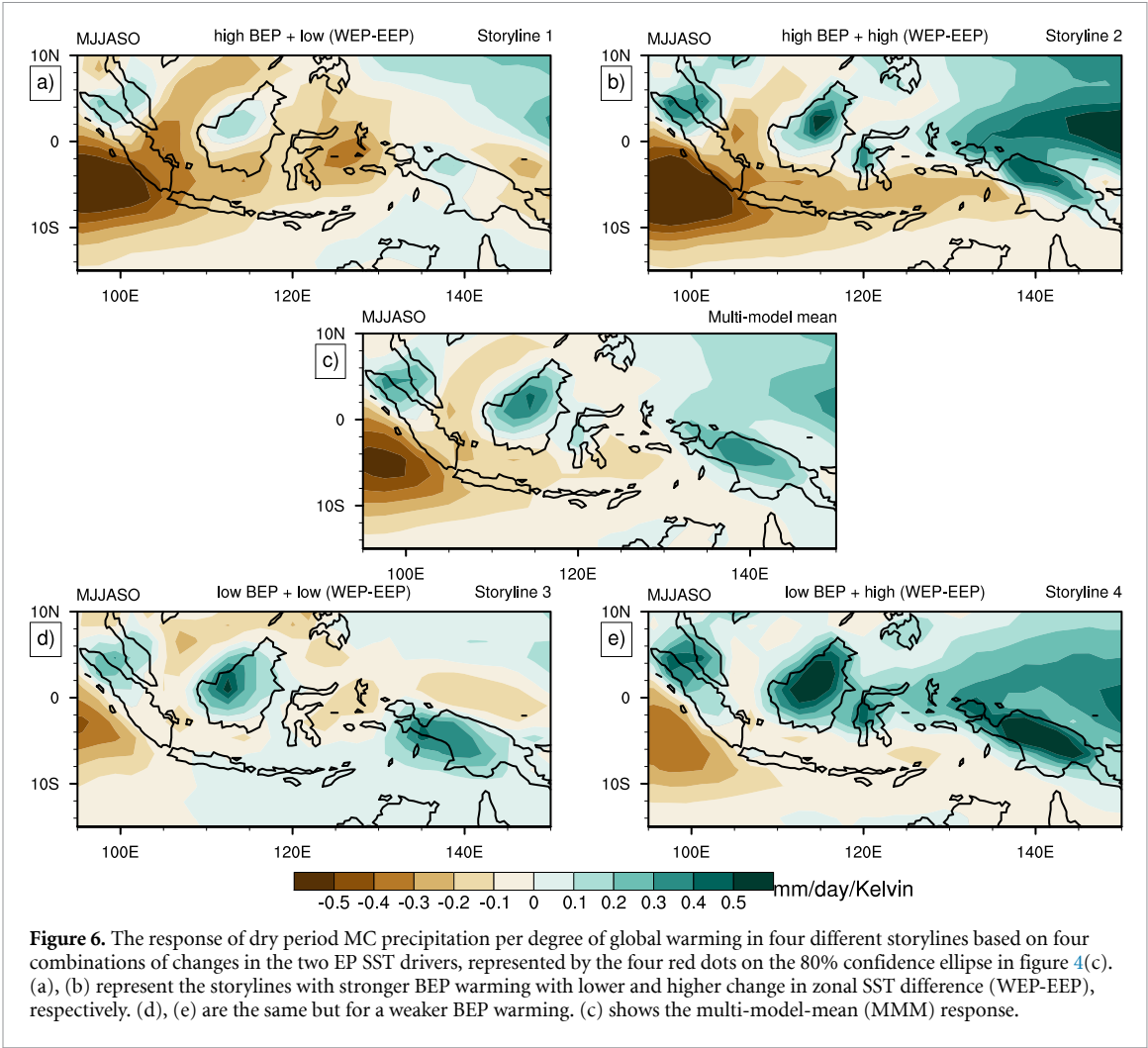
Figure 6. The response of dry period MC precipitation per degree of global warming in four different storylines based on four combinations of changes in the two EP SST drivers, represented by the four red dots on the 80% confidence ellipse in figure 4(c). (a), (b) represent the storylines with stronger BEP warming with lower and higher change in zonal SST difference (WEP-EEP), respectively. (d), (e) are the same but for a weaker BEP warming. (c) shows the multi-model-mean (MMM) response.

Table 1. Over three MC regions (shown in figure 5), area averaged precipitation response (in units of mm d^{-1} K^{-1}) to each driver and for the four storylines shown in figure 6 along with the median absolute deviation of the residuals (ResMAD) from the MLR.

Region	b	c	Storyline1	Storyline2	Storyline3	Storyline4	ResMAD
Sumatra	-0.12	0.03	-0.39	-0.31	-0.06	0.01	0.16
Kalimantan	-0.11	0.06	-0.08	0.07	0.21	0.36	0.10
New Guinea	-0.10	0.13	-0.04	0.28	0.22	0.56	0.16

three key regions in the MC (shown as dashed black boxes in figure 5) along with the median absolute deviation of the residuals (ResMAD) from the MLR equation (1) (table 1). The ResMAD indicates the noise level in the MLR model. We find that the differences in the area averaged storyline values over these regions are larger than the ResMAD, indicating the robust explanatory potential of the storylines.

4. Conclusions

Utilising the uncertainty of the EP SST evolution in the CMIP6 models, we construct storylines of how the future EP SST changes could influence the MC dry period precipitation under global warming. We find that a BEP warming leads to a drying response over the south-western MC regions of Sumatra, Java and Kalimantan. We also find that a positive change in the WEP-EEP SST difference leads to more precipitation over northern Borneo, Sulawesi and New Guinea.

Our findings suggest that the CMIP6 MMM response of future drying over the south-western part of the MC is linked with the BEP warming. Previous studies with CMIP5 models and regional climate models also found such a drying response over the MC, especially over central to southern Sumatra and Java (Giorgi *et al* 2019, Supari *et al* 2020, Tangang *et al* 2020). These studies suggest that such a drying response could be related to changes in the Hadley circulation (Fu 2015, Laua and Kim 2015) or to changes in the North Pacific subtropical high (He and Zhou 2015, He *et al* 2015, Fu and Guo 2020) under global

warming. Further research is needed to investigate the causal relationship between these different aspects of the climate system.

Our focus here is on the EP SST as the main driver of uncertainty in changes in MC dry period rainfall. However, it must be noted that there are other potential drivers such as the equatorial Indian Ocean SST which could also explain some of the uncertainty in MC dry period rainfall changes. We find a large model uncertainty in future Indian Ocean dipole-like SST evolution, represented as the difference between western and eastern equatorial Indian Ocean (WEI-EEI) SST (figure S3(a)). The spatial pattern of this model uncertainty shows a prominent negative SST anomaly over EEI, adjacent to Sumatra (figure S3(b)). We have tested for a potential confounding influence from this WEI-EEI SST uncertainty on the relation found here between EP SST and MC dry period precipitation changes by regressing out the influence of the WEI-EEI SST changes on the MC precipitation changes before applying the MLR model (in equation (1)). That procedure led to the same results as in figure 5, showing that there is no confounding influence of WEI-EEI SST uncertainty on our findings. To quantify the additional influence of the WEI-EEI SST uncertainty on the MC dry period precipitation changes, we regress the residual from the MLR model (in equation (1)) on the WEI-EEI SST changes. We find a significant drying response over southern Sumatra and Java (figure S3(c)), which explains 20% to 30% of the total variance in the future precipitation changes over this region (figure S3(d)). Hence, for assessing future risks over southern Sumatra and Java, accounting for changes in the equatorial Indian Ocean SST driver would be important.

Previous studies have suggested potential biases in the ability of climate models to simulate centennial time scale changes in the tropical Pacific SST (Samanta *et al* 2018), and also to simulate the observed tropical SST climatology which links to the known biases in the Intertropical Convergence Zone (Samanta *et al* 2019). Reducing these biases could potentially reduce the uncertainty in the model projected tropical Pacific SST and also in the associated dry period rainfall over the MC. From previous phases of the CMIP, a gradual improvement in representing the mean state of the tropical Pacific SST has been found (Bellenger *et al* 2014, Jiang *et al* 2021), with improved associated rainfall teleconnections (Grose *et al* 2020). Recent studies suggest that moving towards high resolution model simulations with resolved ocean mesoscale eddies could further reduce the remaining biases in the tropical Pacific SST (Wengel *et al* 2021, Liu *et al* 2022). Such improvements could potentially constrain the plausibility of some of the storylines described here.

Our storylines suggest that for a high BEP warming, the south-western MC could face drier conditions enhancing the future possibilities of severe forest fires. However, the observed record over the last 119 years suggests a moderate to low BEP warming compared to the spread in the CMIP6 models over the same period (figure S1). Furthermore, the observed WEP minus EEP SST trend shows a high positive value compared to the historical trends in the models (figure S1). A recent review on the understanding of the tropical Pacific zonal SST gradient suggests that such a difference between the observations and the models reflects either an error in the models to simulate the forced response or the models' underestimation in simulating multidecadal scale variability over the tropical Pacific (Lee *et al* 2022). Therefore, a continuation of the observed trend in the zonal SST gradient for the future is indeed a possibility. Through the storyline method, we are able to avoid the risk of not addressing such a potential future evolution in tropical Pacific SST and can indicate that under the condition of a continued observed WEP-EEP SST trend, a storyline with high precipitation over the north-eastern parts of the MC could be realised.

Data availability statement

Acknowledgments

ORCID iD

Rohit Ghosh ⦿ https://orcid.org/0000-0001-9888-7292

References

Becker A, Finger P, Meyer-Christoffer A, Rudolf B, Schamm K, Schneider U and Ziese M 2013 A description of the global land-surface precipitation data products of the Global Precipitation Climatology Centre with sample applications including centennial (trend) analysis from 1901-present *Earth Syst. Sci. Data* **5** 71–99

Bellenger H, Guilyardi E, Leloup J, Lengaigne M and Vialard J 2014 ENSO representation in climate models: from CMIP3 to CMIP5 *Clim. Dyn.* **42** 1999–2018

Chang C P, Wang Z, Ju J and Li T 2004 On the relationship between western Maritime Continent monsoon rainfall and ENSO during northern winter *J. Clim.* **17** 665–72

IOP Publishing ·

Environ. Res. Lett. **18** (2023) 034017 · R Ghosh and T G Shepherd

Chang C-P, Wang Z, McBride J and Liu C-H 2005 Annual cycle of Southeast Asia—Maritime Continent rainfall and the asymmetric *J. Clim.* **18** 287–301

Eyring V, Bony S, Meehl G A, Senior C A, Stevens B, Stouffer R J and Taylor K E 2016 Overview of the Coupled Model Intercomparison Project Phase 6 (CMIP6) experimental design and organization *Geosci. Model Dev.* **9** 1937–58

Fu R 2015 Global warming-accelerated drying in the tropics *Proc. Natl Acad. Sci. USA* **112** 3593–4

Fu Y and Guo D 2020 Projected changes in the western North Pacific subtropical high under six global warming targets *Atmos. Ocean. Sci. Lett.* **13** 26–33

Ge F, Zhu S, Luo H, Zhi X and Wang H 2021 Future changes in precipitation extremes over Southeast Asia: insights from CMIP6 multi-model ensemble *Environ. Res. Lett.* **16** 024013

Ghosh R 2023 CMIP6 data for the analysis in the article "Storylines of Maritime Continent dry period precipitation changes under global warming" (Zenodo) (https://doi.org/10.5281/zenodo.7589057)

Giorgi F, Raffaele F and Coppola E 2019 The response of precipitation characteristics to global warming from climate projections *Earth Syst. Dyn.* **10** 73–89

Grose M R *et al* 2020 Insights from CMIP6 for Australia's future climate *Earths Future* **8** e2019EF001469

Haylock M and McBride J 2001 Spatial coherence and predictability of Indonesian wet season rainfall *J. Clim.* **14** 3882–7

He C and Zhou T 2015 Responses of the western North Pacific subtropical high to global warming under RCP4.5 and RCP8.5 scenarios projected by 33 CMIP5 models: the dominance of tropical Indian Ocean-tropical western Pacific SST gradient *J. Clim.* **28** 365–80

He C, Zhou T, Lin A, Wu B, Gu D, Li C and Zheng B 2015 Enhanced or weakened western north pacific subtropical high under global warming? *Sci. Rep.* **5** 1–7

Hendon H H 2003 Indonesian rainfall variability: impacts of ENSO and local air-sea interaction *J. Clim.* **16** 1775–90

Huijnen V, Wooster M J, Kaiser J W, Gaveau D L A, Flemming J, Parrington M, Inness A, Murdiyarso D, Main B and Van Weele M 2016 Fire carbon emissions over Maritime Southeast Asia in 2015 largest since 1997 *Sci. Rep.* **6** 1–8

Jiang N and Zhu C 2020 Tropical Pacific cold tongue mode triggered by enhanced warm pool convection due to global warming *Environ. Res. Lett.* **15** 054015

Jiang W, Huang P, Huang G and Ying J 2021 Origins of the excessive westward extension of ENSO SST simulated in CMIP5 and CMIP6 models *J. Clim.* **34** 2839–51

Johnston F H, Henderson S B, Chen Y, Randerson J T, Marlier M, DeFries R S, Kinney P, Bowman D M J S and Brauer M 2012 Estimated global mortality attributable to smoke from landscape fires *Environ. Health Perspect.* **120** 695–701

Juneng L and Tangang F T 2005 Evolution of ENSO-related rainfall anomalies in Southeast Asia region and its relationship with atmosphere—Ocean variations in Indo-Pacific sector *Clim. Dyn.* **25** 337–50

Kang S, Im E-S and Eltahir E A B 2019 Future climate change enhances rainfall seasonality in a regional model of western Maritime Continent *Clim. Dyn.* **52** 747–64

Kim P S, Jacob D J, Mickley L J, Koplitz S N, Marlier M E, DeFries R S, Myers S S, Chew B N and Mao Y H 2015 Sensitivity of population smoke exposure to fire locations in Equatorial Asia *Atmos. Environ.* **102** 11–17

Koplitz S N *et al* 2016 Public health impacts of the severe haze in Equatorial Asia in September-October 2015: demonstration of a new framework for informing fire management strategies to reduce downwind smoke exposure *Environ. Res. Lett.* **11** 1–10

Kubota H, Shirooka R, Jun-Ichi H and Syamsudin F 2011 Interannual rainfall variability over the eastern Maritime Continent *J. Meteorol. Soc. Japan* **89** 111–2

L'Heureux M L, Collins D C and Hu Z Z 2013 Linear trends in sea surface temperature of the tropical Pacific Ocean and implications for the El Niño-Southern Oscillation *Clim. Dyn.* **40** 1223–36

Laua W K M and Kim K M 2015 Robust Hadley circulation changes and increasing global dryness due to CO2 warming from CMIP5 model projections *Proc. Natl Acad. Sci. USA* **112** 3630–5

Lee S, L'Heureux M, Wittenberg A T, Seager R, O'Gorman P A and Johnson N C 2022 On the future zonal contrasts of equatorial Pacific climate: perspectives from observations, simulations, and theories *npj Clim. Atmos. Sci.* **5** 1–15

Lelieveld J, Evans J S, Fnais M, Giannadaki D and Pozzer A 2015 The contribution of outdoor air pollution sources to premature mortality on a global scale *Nature* **525** 367–71

Lestari S, Hamada J I, Syamsudin F, Sunaryo M J and Yamanaka M D 2016 ENSO influences on rainfall extremes around Sulawesi and Maluku islands in the eastern Indonesian Maritime Continent *Sci. Online Lett. Atmos.* **12** 37–41

Lewis N and Curry J A 2015 The implications for climate sensitivity of AR5 forcing and heat uptake estimates *Clim. Dyn.* **45** 1009–23

Li Y, Chen Q L, Li J P, Zhang W J, Song M H, Hua W, Cai H K and Wu X F 2019 The tropical Pacific cold tongue mode and its associated main ocean dynamical process in CMIP5 models *Earth Planet. Phys.* **3** 400–13

Li Y, Li J, Zhang W, Chen Q, Feng J, Zheng F, Wang W and Zhou X 2017 Impacts of the Tropical Pacific cold tongue mode on ENSO diversity under global warming *J. Geophys. Res. Oceans* **122** 8524–42

Li Y, Li J, Zhang W, Zhao X, Xie F and Zheng F 2015 Ocean dynamical processes associated with the tropical Pacific cold tongue mode *J. Geophys. Res. Oceans* **120** 6419–35

Liu B, Gan B, Cai W, Wu L, Geng T, Wang H, Wang S, Jing Z and Jia F 2022 Will increasing climate model resolution be beneficial for ENSO simulation? *Geophys. Res. Lett.* **49** e2021GL096932

Margono B A, Potapov P V, Turubanova S, Stolle F and Hansen M C 2014 Primary forest cover loss in Indonesia over 2000-2012 *Nat. Clim. Change* **4** 730–5

Marlier M E, Defries R S, Voulgarakis A, Kinney P L, Randerson J T, Shindell D T, Chen Y and Faluvegi G 2013 El Niño and health risks from landscape fire emissions in Southeast Asia *Nat. Clim. Change* **3** 131–6

McBride J L, Haylock M R and Nicholls N 2003 Relationships between the Maritime Continent heat source and the El Niño-Southern oscillation phenomenon *J. Clim.* **16** 2905–14

Mindlin J, Shepherd T G, Vera C S, Osman M, Zappa G, Lee R W and Hodges K I 2020 Storyline description of southern hemisphere midlatitude circulation and precipitation response to greenhouse gas forcing *Clim. Dyn.* **54** 4399–421

Murakami T and Sumi A 1978 Southern hemisphere summer monsoon circulation during the 1978-79 WMONEX part I : monthly mean wind fieldsi1 *J. Meteorol. Soc. Japan* **60** 638–48

Nichol J 1998 Smoke haze in Southeast Asia: a predictable recurrence *Atmos. Environ.* **32** 2715–6

Page S E, Siegert F, Rieley J O, Boehm H D V, Jaya A and Limin S 2002 The amount of carbon released from peat and forest fires in Indonesia during 1997 *Nature* **420** 61–65

Qian J H 2008 Why precipitation is mostly concentrated over islands in the Maritime Continent *J. Atmos. Sci.* **65** 1428–41

Rayner N A, Parker D E, Horton E B, Folland C K, Alexander L V, Rowell D P, Kent E C and Kaplan A 2003 Global analyses of sea surface temperature, sea ice, and night marine air temperature since the late nineteenth century *J. Geophys. Res. Atmos.* **108** 4407

Reid J S, Xian P, Hyer E J, Flatau M K, Ramirez E M, Turk F J, Sampson C R, Zhang C, Fukada E M and Maloney E D 2012 Multi-scale meteorological conceptual analysis of observed active fire hotspot activity and smoke optical depth in the Maritime Continent *Atmos. Chem. Phys.* **12** 2117–47

Roxy M K, Dasgupta P, McPhaden M J, Suematsu T, Zhang C and Kim D 2019 Twofold expansion of the Indo-Pacific warm pool warps the MJO life cycle *Nature* **575** 647–51

Samanta D, Karnauskas K B and Goodkin N F 2019 Tropical Pacific SST and ITCZ biases in climate models: double trouble for future rainfall projections? *Geophys. Res. Lett.* **46** 2242–52

Samanta D, Karnauskas K B, Goodkin N F, Coats S, Smerdon J E and Zhang L 2018 Coupled model biases breed spurious low-frequency variability in the tropical Pacific Ocean *Geophys. Res. Lett.* **45** 10,609–18

Schneider U, Finger P, Meyer-Christoffer A, Rustemeier E, Ziese M and Becker A 2017 Evaluating the hydrological cycle over land using the newly-corrected precipitation climatology from the Global Precipitation Climatology Centre (GPCC) *Atmosphere* **8** 52

Seager R, Cane M, Henderson N, Lee D E, Abernathey R and Zhang H 2019 Strengthening tropical Pacific zonal sea surface temperature gradient consistent with rising greenhouse gases *Nat. Clim. Change* **9** 517–22

Shepherd T G *et al* 2018 Storylines: an alternative approach to representing uncertainty in physical aspects of climate change *Clim. Change* **151** 555–71

Supari T F *et al* 2020 Multi-model projections of precipitation extremes in Southeast Asia based on CORDEX-Southeast Asia simulations *Environ. Res.* **184** 109350

Supari T F, Salimun E, Aldrian E, Sopaheluwakan A and Juneng L 2018 ENSO modulation of seasonal rainfall and extremes in Indonesia *Clim. Dyn.* **51** 2559–80

Tangang F *et al* 2020 Projected future changes in rainfall in Southeast Asia based on CORDEX–SEA multi-model simulations *Clim. Dyn.* **55** 1247–67

Tangang F, Latif M T and Juneng L 2010 Climate change: is Southeast Asia up to the challenge?: The roles of climate variability and climate change on smoke haze occurrences in Southeast Asia region *LSE IDEAS, London Sch. Econ. Polit. Sci.* pp 36–49

Tebaldi C and Arblaster J M 2014 Pattern scaling: its strengths and limitations, and an update on the latest model simulations *Clim. Change* **122** 459–71

Wengel C, Lee S S, Stuecker M F, Timmermann A, Chu J E and Schloesser F 2021 Future high-resolution El Niño/Southern Oscillation dynamics *Nat. Clim. Change* **11** 758–65

Wills R C J, Dong Y, Proistosecu C, Armour K C and Battisti D S 2022 Systematic climate model biases in the large-scale patterns of recent sea-surface temperature and sea-level pressure change *Geophys. Res. Lett.* **49** e2022GL100011

Yang Y M, Park J H, Il A S, Wang B and Luo X 2021 Mean sea surface temperature changes influence ENSO-related precipitation changes in the mid-latitudes *Nat. Commun.* **12** 1–9

Zappa G, Bevacqua E and Shepherd T G 2021 Communicating potentially large but non-robust changes in multi-model projections of future climate *Int. J. Climatol.* **41** 3657–69

Zappa G and Shepherd T G 2017 Storylines of atmospheric circulation change for European regional climate impact assessment *J. Clim.* **30** 6561–77

Zhang T, Yang S, Jiang X and Huang B 2016 Roles of remote and local forcings in the variation and prediction of regional Maritime Continent rainfall in wet and dry seasons *J. Clim.* **29** 8871–9

Zhang W, Li J and Zhao X 2010 Sea surface temperature cooling mode in the Pacific cold tongue *J. Geophys. Res. Oceans* **115** 1–15